STUDY ON MICROSTRUCTURE AND WEAR PROPERTIES OF GRAPHENE AND SICP HYBRID REINFORCED ALUMINUM MATRIX COMPOSITES

X. M. DU[a], G. S. FANG[a], J. B. GAO[b], H. T. QI[a], K. F. ZHENG[a], S. GUO[a], G. S. GUO[a]*, F. G. LIU[a]

[a] *School of Materials Science and Engineering, Shenyang Ligong University, Shenyang 110159, China*.

[b] *Centre of Excellence for Advanced Materials, Dongguan 523808, China.*

Graphene and SiC nanoparticles hybrid reinforced aluminum matrix composites were prepared by ball milling and hot press sintering. The effect of graphene content on microstructure and wear properties of composites was investigated. The results show that increasing the graphene content is beneficial to maintain the structural integrity of graphene during ball milling and hot pressing sintering, and to reduce the stress concentration of SiC nanoparticles on the matrix. The wear resistance of the composite is improved with the increase of graphene content. As the graphene content increases, the wear mechanism changes from abrasive wear to delamination wear. Through the analysis of the cross-sectional morphology of the wear marks, it is found that the improvement of the wear resistance is based on the formation of a graphene-rich dry lubricating layer on the worn surface, which explains the formation mechanism of the graphene dry lubricating layer in the composite.

(Received January 6, 2020; Accepted May 25, 2020)

Keywords: Graphene, SiC nanoparticle, Aluminum matrix composite, Microstructure, Wear properties

1. Introduction

Graphene is a kind of two-dimensional honeycomb crystal structure nanomaterials composed of carbon atoms[1]. Graphene is considered to be an ideal reinforcing material because of its excellent intrinsic mechanical properties [2] and good lubrication properties [3].In recent years, it has been widely used in the research of metal matrix composites [4-6]. With the ultra-low friction coefficient of graphene being reported [7], many researchers have paid much attention to the tribological properties of graphene reinforced metal matrix composites. Zhai et al. [8]prepared GNPs/Ni_3Al composites and tested their friction and wear properties. The results showed that GNPs, as an effective solid lubricant, can form a protective layer during sliding, which reduce the wear rate and friction coefficient. Li et al.[9] investigated the tribological properties of graphene/copper composites and graphite/copper composites. The results showed that graphene will gradually form a wear resistant layer in the process of wear, which has a protective effect on the matrix material. The graphene/copper composites have higher wear resistance and lower friction coefficient than that of graphite/copper composites.

Recently, with the research on the tribological properties of composites, a concept of tribological material design has been gradually recognized, that is the composite reinforcement phase of soft particle lubrication and hard particle strengthening [10].For example, SiC-CNT [11],

*Corresponding author: 1013508301@qq.com

SiC-graphite [12, 13], Al_2O_3-graphite [14, 15] and B_4C-graphite [16]. The combination of these reinforcements can effectively enhance the mechanical properties and wear properties of aluminum-based and copper-based composites. This combination breaks the agglomeration phenomenon of soft particles in the preparation process, so that the reinforcement phase can be evenly distributed to obtain better performance. However, at present, there are few studies on graphene and ceramic particles hybrid reinforced aluminum alloy matrix, and the effect of this hybrid reinforcement on the microstructure, mechanical properties and wear behavior of aluminum matrix composites is still unclear.

In this paper, SiC nanoparticles and graphene were used as reinforcements, Al7075 matrix composites were prepared by high-energy ball milling and vacuum hot pressing, and their microstructure, hardness, friction and wear behavior were characterized, in order to study the synergistic strengthening mechanism and tribological properties of graphene and SiC nanoparticles in the composites.

2. Experimental

2.1. Materials

The matrix material is Al7075 (Al-Zn-Mg-Cu alloy) powder (10 μm, provided by Beijing Hongyu Materials Co., Ltd.). Graphene and SiC nanoparticles (800 nm, supplied by Shanghai Yunfu Nano Technology Co., Ltd.) are used as reinforcement phase. The graphene is the commercial agent of Nanjing XFNANO material Technology Co., Ltd. All the above materials can be used without further purification.

The three samples were prepared by ball milling mixing and vacuum hot pressing sintering. Detailed preparation methods have been documented in previous studies[17]. They have the same SiC content (0.25%) and different graphene content, which are 0% (AS), 0.25% (ASG1) and 0.50% (ASG2), respectively.

All the composite samples were treated with solid solution at 470 ℃ for 2 h, and then quenched in cold water. The quenched samples were aged for 16 hours at 140 ℃.

2.2. Microstructure

The X-ray diffraction pattern of graphene and SiC were recorded on Rigaku Ultima IV X-ray diffractometer using Cu Kα (λ=1.54060Å) radiation. The selected diffraction peaks were slowly scanned (4°/min) in step mode. The step size is 0.02°. The diffraction angle (2θ) was maintained between 20° and 100°.

The surface morphologies of the three samples were observed by scanning electron microscope (SEM) of TESCAN equipped with energy dispersive spectroscopy (EDS). The relative density was determined by Archimedes method. The relative densities of the three samples were calculated by using the composite mixing rule.

Graphene and its structural changes during sintering were studied by Raman spectroscopy using a Jobin-Yvon microspectrometer (LabRam HR, Jobin-YvonCo. Ltd., France). Under environmental conditions, the spectra were collected by 514.5 nm lines of argon ion laser. The Vickers hardness of the sample was measured by Vickers hardness tester (HVS- 50,Shanghai, China). The load was 9.8N and the residence time was 10s, which was measured 10 times in each

sample.

2.3. Dry sliding wear test

The dry sliding wear test was carried out by using reciprocating friction and wear tester (MDW-02, Jinan, China). All samples are carefully polished to reach mirror like surface finish (Ra = 0.1μm) before all the tests. The GCr15 bearing steel ball (HRC63 ±3) with a diameter of 6.35 mm was used as the friction pair to carry out the wear test. The dry wear test was carried out under 10N load at room temperature. These wear tests were carried out at the sliding speed of 0.02m/s with a reciprocating stroke of 0.01m and lasted for 20 minutes. The total sliding distance is 24 m.The specific wear rate [18,19] was calculated as:

$$W = \frac{V}{F_N S} \tag{1}$$

where V (m^3) is the wear volume loss after the sliding test, F_N (N) is the normal load and S (m) is the sliding distance.

The wear surface were observed and analyzed by scanning electron microscope (SEM).The depth, width and roughness of wear marks were analyzed by laser scanning confocal microscope(LSCM) (LEXT OLS4100,Japan).

3. Resultsand discussion

Fig. 1 shows the morphology of the raw materials and the XRD pattern of the composites. The results indicate that graphene have a two-dimensional high aspect ratio sheet geometry, and the wrinkles and folds is also showed on the exfoliated graphene sheet. The graphene consisted of platelets with the morphology of irregular shaped flakes with mean diameters less than 5-10 μm and its thickness is 3-10nm, corresponding to approximately 10-50 sheets of graphene (Fig. 1a). The SiC nanoparticles are sharp and angular (Fig. 1b). The mean size of the particles appears to be ～1um (Fig.1b). The X-ray diffraction patterns of graphene, SiC nanoparticles and hybrid composites with different mass fractions of graphene and SiC nanoparticles are shown in Fig. 1c. As can be seen from the figure, there is a characteristic peak (002) of graphene at 2θ = 26.5°. The diffraction peaks of 2θ at 38.5°, 44.7°, 65.1°, 78.2°, 88.4° and 99.1° are respectively the diffraction peaks of α-Al (111), (200), (220), (311), (222) and (400). In addition, no SiC XRD diffraction peak was observed in all samples, and only a weak graphene diffraction peak was observed in ASG2 samples. This is because the contents of graphene and SiC nanoparticles in the composites are relatively small, so it is difficult for XRD to detect these low-content reinforcement phases. It should be noted that no aluminum carbide (Al_4C_3) peak was recorded for any of the composite samples. It is believed that there is no chemical reaction between graphene with the Al matrix under this condition. Bartolucci et al. [5] reported the formation of aluminum carbide in graphene/aluminum composites processed by hot extrusion. Bustamante et al. [20] thought that the formation of aluminum carbide has a strong dependence of the processing temperature followed in the production of the composites.

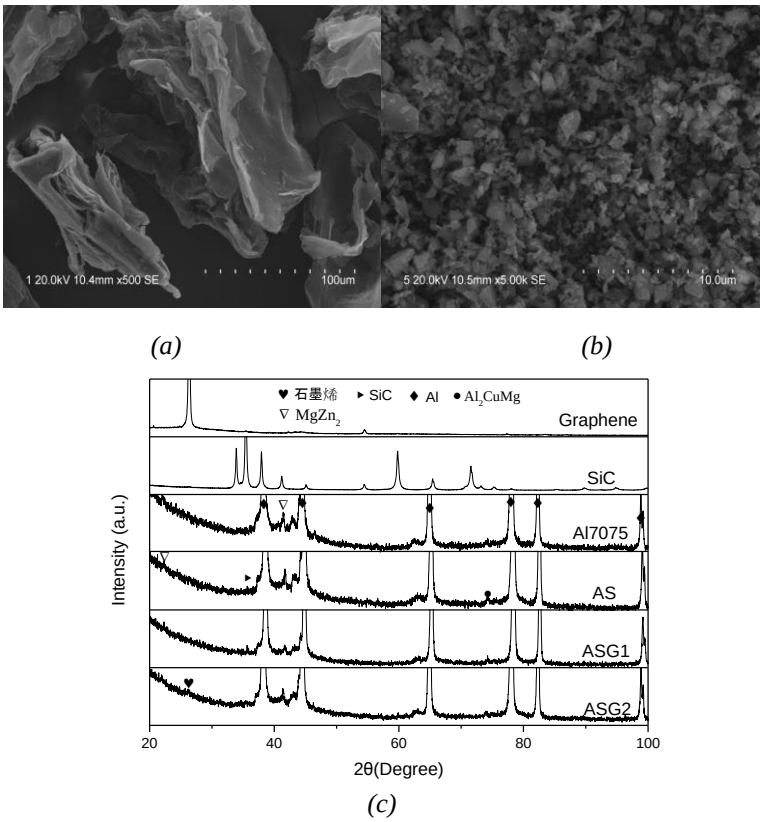

Fig. 1.Microscopic morphology of raw materials and XRD patterns of composite materials (a)Micromorphology of graphene, (b)Micromorphology of SiC nanoparticles and (c) XRD patterns of graphene, SiC nanoparticles and hybrid composites.

SEM micrographs of Al7075/SiCp/graphene nanocomposites with different graphene contents are shown in Fig. 2.When the graphene content in the composite is 0 wt%, SiC particles are uniformly distributed on the boundary of aluminum grains, as shown in Fig.2a. When the mass fraction of graphene in the composite is 0.25wt.% and 0.5wt.%, graphene and SiC nanoparticles can be uniformly distributed at the boundary of aluminum grains and closely connected with the aluminum matrix. Through the EDS analysis of the three samples, it can be found that the distribution of the reinforcement phase is at the boundary of the aluminum grain. The difference is that when graphene is added, the number of SiC nanoparticles at the grain boundaries decreases. Some SiC nanoparticles are coated with graphene, which can improve the wettability of the interface between SiC particles and aluminum matrix, thus improve the uniform dispersion of SiC particles in the matrix alloy, and weaken the stress concentration caused by the sharp corner of SiC nanoparticles to the aluminum matrix to some extent. Since there is no Al_4C_3 brittle phase at the interface between matrix and reinforcement in the aforementioned XRD and SEM analysis, it can be inferred that there is a good interfacial bonding between aluminum matrix and reinforcement phase. In addition, the local aggregation of graphene and SiC nanoparticles at the grain boundary was not found, indicating that graphene plays a key role in the uniform dispersion of SiC particles.

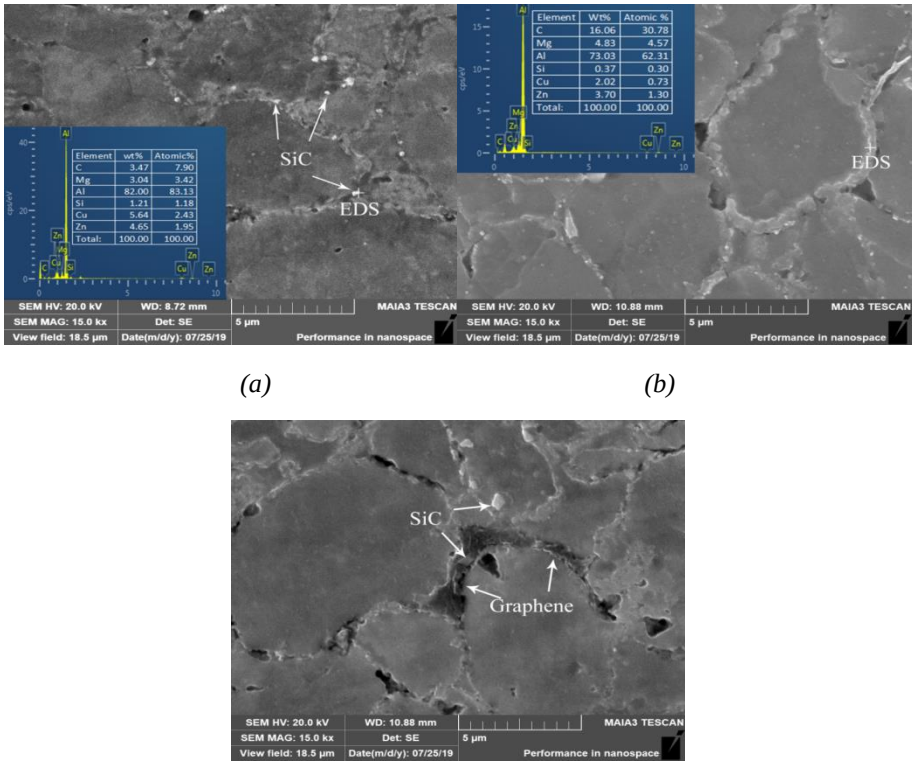

(a) *(b)*

(c)

Fig. 2.SEM micrographs of Al7075/SiCp/graphene composites with different graphene contents:(a) AS; (b) ASG1; (c) ASG2. Inset of (a) and (b) are the EDS results of the corresponding area.

Raman spectroscopy can detect the disorder in graphene by defect activation peak [21]. Raman spectroscopy was used to characterize the structure of original graphene and graphene in ASG1 and ASG2 after ball milling and hot pressing sintering. As clearly shown in Fig. 3, there were three peaks located at ~1360 cm^{-1} (D band), ~1591 cm^{-1} (G band) and ~2763 cm^{-1} (2D band), respectively. The D band is due to out of plane breathing mode of sp2 atoms and the G peak corresponds to the E_{2g} phonon at the Brillouin zone center [22]. And the 2D band is shape of the second-order Raman bands [23]. Moreover the increase in the graphene weight percent did not cause a change in the peak position owing to the same duration of ball-milling in all samples.

When studying the disorder of graphene by Raman spectroscopy, The intensity ratio of D and G peaks (I_D/I_G), which is essential for the characterization of graphene disorder and other attributes [9,24], is given for all samples in Fig.3. As can be seen from Fig. 3, compared with the original graphene, the I_D/ I_G value of ASG1 increased from 1.00 to 1.16, and the I_D/ I_G value of ASG2 increases from 1.00 to 1.13. A slight increase in I_D/ I_G indicates that the structure of graphene is successfully retained with minimal damage during ball milling and sintering. It can be explained by the destruction of C=C aromaticity and the disappearance of sp2 carbon hexagonal structure [21]. At the same time, the I_D/ I_G value of ASG2 is lower than that of ASG1, which indicates that the increase of graphene content in the matrix is helpful to maintain the integrity of its structure.

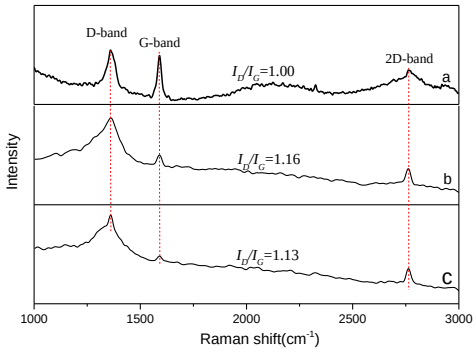

Fig. 3.Raman spectra of (a)graphene, (b) ASG1 and (c) ASG2.

Table 1 summarizes the relative density and Vickers Hardness of the three composites. The relative density of all composite samples is more than 99%, indicating that the composites are dense and have low porosity. It can also be seen from Table 1 that the hardness of the composite sample is obviously higher than that of the pure Al7075 sample. It is worth noting that the hardness of ASG2 sample was 127.8 ± 5.47 HV, showing 38.9% increments over the unreinforced aluminum under otherwise identical experimental conditions. This is mainly due to the following reasons: (1) Due to the coexistence of SiC nanoparticles and graphene in the composites, nano-structured graphene and SiC nanoparticles can inhibit grain growth in aluminum matrix through grain boundary pinning and therefore lead to a finer grain structure of aluminum. Finer grain structures can result in higher hardness [25]. (2) The effect of the difference in the coefficient of thermal expansion (CTE) of the matrix and that of the reinforcements on the hardness of the composite, coefficient of thermal expansion mismatch between graphene, SiC nanoparticles and Al7075, may result in multidirectional thermal stress at graphene-Al interface and improvement of dislocation densities, which will increase the hardness [11]. (3) It is generally believed that because SiC particles are harder than Al7075 particles, their inherent hardness properties are endowed with soft matrix, which makes the matrix obtain higher hardness [26].However, the addition of graphene decreased the hardness of the composites from 116.46HV to 112.14HV, and then increased to 127.80HV. Up to now, the effect of graphene on the hardness of metal matrix composites is not completely clear [27].

Table 1.Relative density and Vickers hardness of samples.

Sample	Relative density(%)	Hardness (HV)
AS	99.4	116.46±7.60
ASG1	99.4	112.14±5.38
ASG2	99.2	127.80±5.47
Al7075	-	92±4.60[17]

Fig.4 shows the graphs of wear curves for Al7075/SiC/graphene nanocomposites with 0.25 wt% SiC - various graphene weight fractions. In this work, wear rate is calculated after a

sliding time period of 20 min for all the samples at a constant sliding velocity. Graphene weight fraction is a major factor influencing the wear rate of the composites, as shown in Fig. 4a. It indicates that the wear rates of the composites with different percentage graphene (0.25 and 0.5 wt%) are less than that of the composite without graphene. Further, while increasing the graphene content significant decrease in the wear rate was observed. This reduction in the wear rate is attributed to the strengthening of composites by an addition of graphene and its tribological properties which forms the thin dry lubricant layer between mating metal. This behavior is in consistent with the work done by the other researchers [28, 29].Fig.4b and Fig.4c show the width and depth of wear tracks of the composite, respectively. With the increase of graphene content, the wear tracks become wider and shallower on the surface of the composites, meaning that the amount of debris in composites is decreasing with the increase of graphene content. This also indicates that the addition of graphene improves the wear resistance of the composites. The coefficient of friction and worn surface roughness are shown in Fig. 4d and Fig. 4e, respectively. It is found that the coefficient of friction and worn surface roughness decrease with the increase of graphene content.

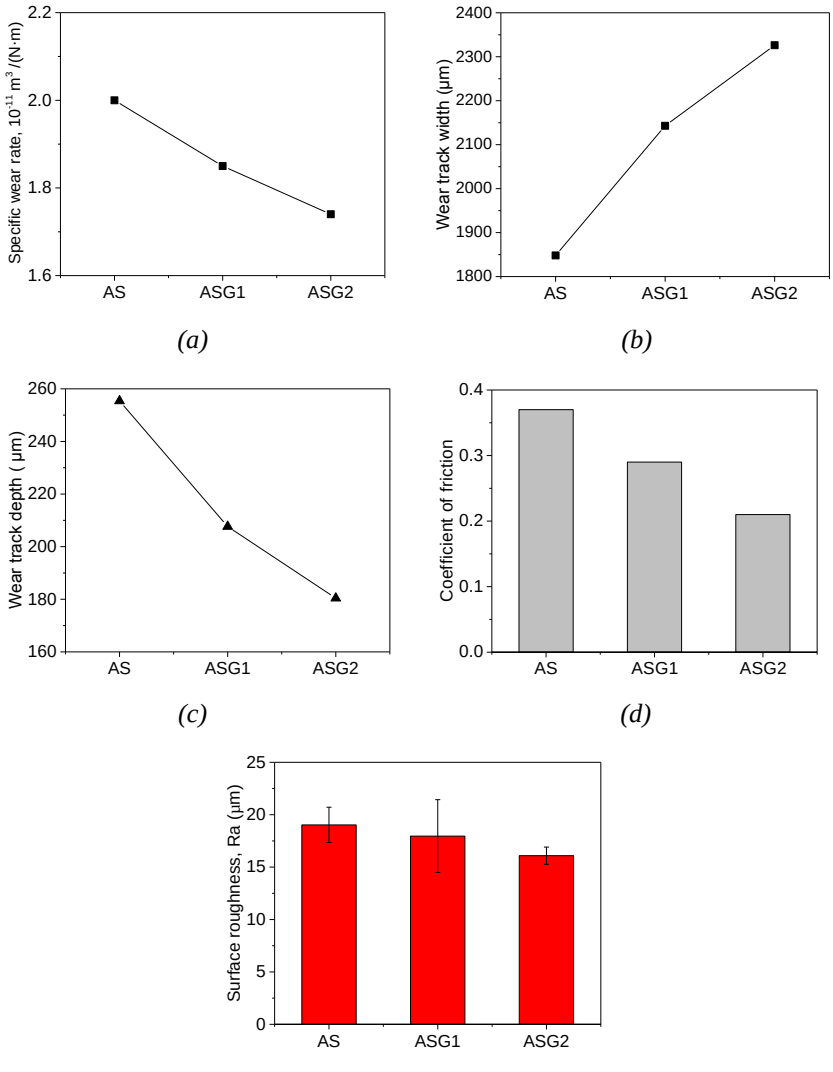

Fig. 4.Tribological properties of AS, ASG1 and ASG2: (a) Specific wear rate, (b) Wear track width, (c) Wear track depth, (d) Coefficient of friction, (e) Roughness of worn surfaces.

Fig. 5 shows the SEM morphology of the worn surface of the composite. Comparing Figs. 5a, 5b and 5c, it can be found that there are more furrows in fig. 5a, and the number of furrows decreases with the increase of graphene content. In addition, a large amount of wear debris can be seen adhering to the worn surface in fig. 5a, and the amount of wear debris is much more than that in figs. 5b and 5c. These wear debris are caused by the plastic deformation of the matrix during sliding wear. Graphene is gradually exposed to the worn surface due to plastic deformation and slowly compacted under wear load to form a thin friction layer [9]. This explains that the composites with graphene have lower friction coefficient. The formation of furrows on the worn surface is related to the mechanism of abrasive wear [13]. In addition, the local area of the worn surface shows material flow along the sliding direction and spalling direction, which indicates the existence of delamination wear mechanism [30]. Therefore, the wear mechanism of the composites is mainly abrasive wear and delamination wear, and with the increase of graphene content, the wear mechanism of the composites changes from abrasive wear to delamination wear.

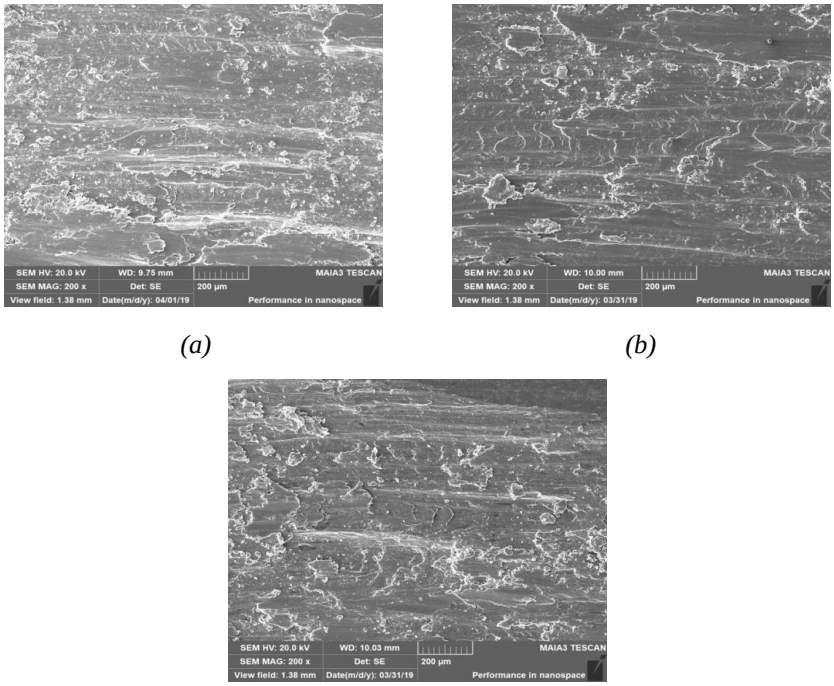

(a) *(b)*

(c)

Fig. 5.SEM micrographs of the worn surface of (a) AS, (b) ASG1, (c) ASG2.

Fig. 6 shows the longitudinal-section and cross-section of the worn surface. The EDS results of longitudinal section show that graphene is enriched and mixed in Al matrix below the worn surface. At the same time, a lot of graphene flakes can be seen in the cross section of the worn surface, which also provides evidence for the existence of graphene dry lubrication layer.

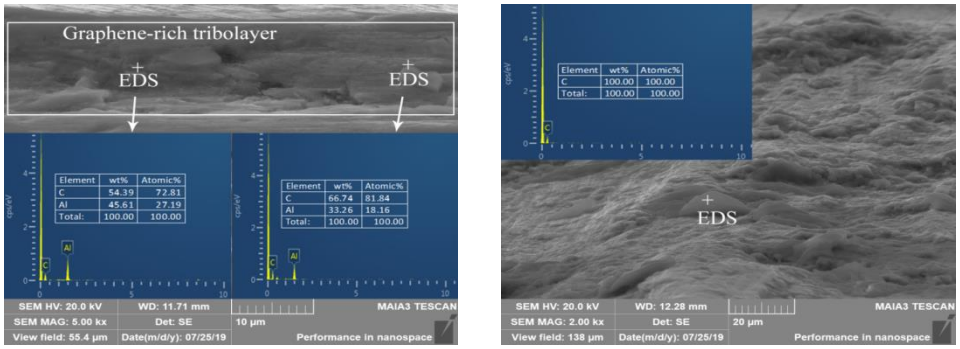

(a) *(b)*

Fig. 6.(a) A SEM micrograph of the longitudinal-section of a worn surface of ASG2, (b)A SEM micrograph of the cross-section of a worn surface of ASG2.

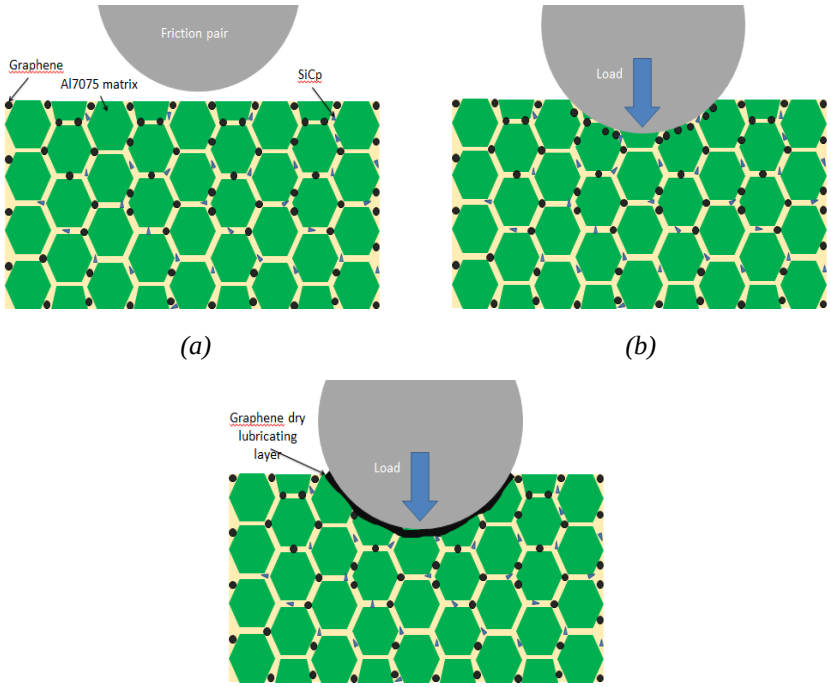

(a) *(b)*

(c)

Fig. 7.The schematic of tribolayer formation of Al7075/SiCp/graphene hybrid composites.

Fig. 7 shows a schematic diagram of dry lubrication layer formation of Al7075 / SiCp / graphene hybrid composites. Initially, graphene and SiCp are uniformly dispersed in the Al7075 matrix (Fig. 7a), and when the sliding wear begins, the friction pair enters the composite under normal load. Graphene and SiCp are gradually exposed to the worn surface due to plastic deformation (Fig. 7b). Because of its lubricity and large specific surface area, graphene is compressed under load and entrapped with some wear debris. As wear develops, more graphene accumulates on the worn surface to form a dry lubrication layer (Fig. 7c).

4. Conclusion

Al7075/SiCp/graphene hybrid reinforced composites were prepared by high energy ball milling and vacuum hot pressing. The effect of graphene content on the microstructure and wear resistance of the composites was studied, and the following conclusions were obtained.

(1) SiC nanoparticles and graphene can be uniformly dispersed in the matrix and distributed at the grain boundary. The increase of graphene content helps to protect the structural integrity of graphene in the matrix and reduce the stress concentration of SiC nanoparticles on the matrix.

(2) With the addition of SiC nanoparticles and graphene, the hardness of the matrix increased obviously and the relative density of the composites decreased.

(3) The wear mechanism of composites mainly includes abrasive wear and delamination wear. With the increase of graphene content, the wear mechanism of the composites changed from abrasive wear to delamination wear.

(4) With the increase of graphene content, the wear resistance of the composites increased, while the friction coefficient and worn surface roughness decreased. Through the analysis of the morphology of the worn surface, the cross section of the worn area and the Raman spectrum of the worn surface, it is confirmed that graphene will gradually form a dry lubricating layer rich in graphene on the worn surface during the wear process.

Acknowledgements

This work was supported by Shenyang Young and Middle-aged Science and Technology Innovation Talents Project (RC180214, RC200355) in Liaoning Province, China and the Program for Guangdong Introducing Innovative and Enterpreneurial Teams (NO: 2016ZT06G025).

References

[1] A. K. Geim, K. S.Novoselov, Nature materials **6**(3), 183(2007).
[2] C. Lee, X. Wei, J. W. Kysar, J. Hone, Science **321**(5887), 385(2008).
[3] D. Berman, A. Erdemir, A. V. Sumant, Materials Today **17**(1), 31(2014).
[4] H. P. Kumar, M. A. Xavior, Procedia Engineering **97**, 1033(2014).
[5] S. F. Bartolucci, J. Paras, M. A. Rafiee, J. Rafiee, S. Lee, D. Kapoor, N. Koratkar, Materials Science and Engineering A **528**, 7933(2011).
[6] R. Pérez-Bustamante, D. Bolaños-Morales, J. Bonilla-Martínez, I. Estrada-Guel, R. Martínez-Sánchez, Journal of alloys and compounds **615**, S578(2014).
[7] Y. J. Shin, R. Stromberg, R. Nay, H. Huang, A. T.S. Wee, H. Yang, C. S. Bhatia, Carbon **49**, 4059(2011).
[8] W. Zhai, X. Shi, M. Wang, Z. Xu, J. Yao, S. Song, Y. Wang, Wear **310**(1-2), 33(2014).
[9] J. Li, L. Zhang, J. Xiao, K. Zhou, Trans. Nonferrous Met. Soc. China **25**(10), 3354(2015).
[10] W. Ames, A. T. Alpas, Metallurgical and Materials Transactions A **26**(1), 85(1995).
[11] M. R. Akbarpour, S. Alipour, A. Safarzadeh, H. S. Kim, Composites Part B **158**, 92(2019).
[12] S. Suresha, B. K. Sridhara, Composites Science and Technology **70**(11), 1652(2010).

[13] A. Vencl, F. Vučetić, B. Bobić, J. Pitel, I. Bobić, Int. J.Adv.Manuf. Technol.**100**, 2135(2018).
[14] M. Kumar, A. M. Murugan, Particulate Science and Technology **37**(3), 261(2019).
[15] A. Baradeswaran, A. E. Perumal, Composites: Part B **56**, 464(2014).
[16] K. Rajkumar, A. Gnanavelbabu, M. S. Venkatesan,K. Rajagopalan, Materials Today: Proceedings **5**(14), 27801(2018).
[17] X. M. Du, K. F. Zheng, T. Zhao, F. G. Liu, Digest Journal of Nanomaterials and Biostructures **13**(4), 1133(2018).
[18] J. Zhang, S. Yang, Z. Chen, H. Wu, J. Zhao, Z. Jiang, Composites Part B **162**, 445(2019).
[19] B. Hekner, J. Myalski, N. Valle, A. Botor-Probierz, M. Sopicka-Lizer, J. Wieczorek, Composites: Part B **108**, 291(2017).
[20] R. Pérez-Bustamante, F. Pérez-Bustamante, I. Estrada-Guel, L. Licea-Jiménez, M. Miki-Yoshida, R. Martínez-Sánchez, Materials Characterization **75**, 13(2013).
[21] S. N. Alam, L. Kumar, Materials Science & Engineering A **667**, 16(2016).
[22] M. Rashad, F. Pan, Z. Yu, M. Asif, H. Lin, R. Pan, Progress in Natural Science: Materials International **25**(5), 460(2015).
[23] S. E. Shin, Y. J. Ko, D. H. Bae, Composites Part B **106**, 66(2016).
[24] J. Liao, M. Tan, Powder Technology **208**(1), 42(2011).
[25] M. R. Akbarpour, E. Salahi, F. A. Hesari, A. Simchi, H. S. Kim, Materials Science & Engineering A **572**, 83(2013).
[26] X. M. Du, K. F. Zheng, F. G. Liu, Digest Journal of Nanomaterials and Biostructures**13**(1), 253(2018).
[27] J. Zhang, S. Yang, Z. Chen, M. Wyszomirska, J. Zhao, Z. Jiang, Tribology International **131**, 94(2019).
[28] H. G. P. Kumar, M. A. Xavior, Procedia engineering **174**, 992(2017).
[29] J. Lin, L. Wang, G. Chen, Tribology letters **41**(1), 209(2011).
[30] M. R. Akbarpour, M. Najafi, S. Alipour, H. S. Kim, Materials Today Communications **18**, 25(2019).